3 Time and Frequency Selective Radio Channel

Small-scale fading, or simply fading, is used to describe the rapid fluctuation of the amplitude of the received radio signal over a short period of time or travel distance, so that large-scale path loss effects (i.e., the variation of the local mean, see chapter 2) may be ignored. Fading is caused by interference between several (two or more) versions of the same transmitted signal (e.g., line-of-sight, reflected, diffracted, and/or scattered signal) which arrive at the receiver at slightly different times. This multipath effect causes the resulting signal at the receiving antenna port to vary widely in amplitude and phase, depending on the distribution of the intensity and relative propagation time of the waves and the bandwidth of the transmitted signal [Rappaport, 1996].

3.1 An Introduction to Small-Scale Fading

Multipath in the radio channel creates *small-scale fading*. The three most important effects are [Geng and Wiesbeck, 1998, Rappaport, 1996]:

- *rapid changes in signal strength* over a small travel distance or time interval,
- *frequency modulation* due to varying *Doppler shifts* on different multipath signals,
- *frequency selectivity* (i.e., dispersion) caused by multipath propagation delays.

For example, for wireless mobile communication systems in built-up urban areas, fading occurs because the height of the mobile antennas are well below the height of the buildings, so there is often no line-of-sight path to the base station (BS). Even when a line-of-sight path exists, multipath still occurs due to reflections/scattering from the ground and buildings. The incoming waves arrive from different directions (AOA: angle of arrival) with, in general, different propagation delays, randomly distributed amplitudes and phases. These multipath components combine vectorially (remember comments on phasor) at the receiver and can cause the received signal to distort or fade. Even when the mobile station (MS) is stationary (i.e., the MS does not move), the signal may fade due to a movement of surrounding objects (e.g., trees, cars, trucks) or changes in the weather conditions (e.g., rain, snow).

If objects are static, and only the mobile receiver is considered to be moving, then fading is purely a spatial phenomenon. The *spatial variations* of the signal (see interference patterns in section 3.5) are seen as *temporal variations* by the receiver as it moves through the interference pattern. The plot in Fig. 2.1 (chapter 2) shows typical rapid variations in the received signal level due to small-scale fading. Due to the relative motion between a mobile receiver and the BS, each multipath wave experiences a shift in frequency, called *Doppler shift*, directly proportional to the velocity and depending on the direction of motion of the MS with respect to the AOA of the individual multipath wave.

Many physical factors in the radio propagation channel influence small-scale fading (for fixed-terminal wireless radio systems, e.g., microwave LOS radio links or stationary reception of TV/radio, only parts of the following list are relevant):

- *Multipath propagation*: The randomly changing amplitudes, phases, and/or AOAs of the waves incident at the receiver location, cause fluctuations in the signal strength, thereby inducing small-scale fading (section 3.2) and/or signal distortion (e.g., signal smearing, intersymbol interference, section 3.4).
- *Speed of the receiver*: The motion of a mobile receiver (e.g., MS in GSM systems) results in random frequency modulation due to different and changing Doppler shifts on the individual multipath components (section 3.5). The frequency shift can be positive or negative depending on whether the receiver is moving towards or away from the fixed BS.
- *Speed of surrounding objects*: If surrounding objects are in motion (e.g., trees, cars, or trucks), they induce changes in the received field strength (section 3.2) as well as time varying Doppler shifts (section 3.5), even for a stationary receiving antenna.
- *The signal bandwidth*: If the signal bandwidth is larger than the “bandwidth” of the channel, the received signal will be distorted (frequency selective fading). As will be shown in section 3.4, the bandwidth of the channel is quantified by the coherence bandwidth, which is a measure of the maximum frequency difference for which signals are still strongly correlated in amplitude (and phase). If the transmitted signal has a narrow bandwidth compared to the so-called Doppler spread (i.e., the width of the spectrum caused by Doppler), then the time fluctuations become important (fast fading, see section 3.5).

3.2 Distribution of the Received Signal Strength

Due to changing amplitudes, phases, and AOAs of the individual multipath components, the received signal (e.g., power, field strength, open-circuit voltage) varies with

time. Here in this section, we are only interested in the *amplitude distribution of the received signal*; a characterization of the temporal changes follows in section 3.5.

The complex open-circuit voltage at the terminals of a receiving antenna is written as:

$$\underline{V}_R(f,t) = V_R(f,t)e^{j\alpha_R(f,t)} = \sum_{i=1}^{N(t)} V_{Ri}(t,f)e^{j\alpha_{Ri}(f,t)} \tag{3.1}$$

where $V_R = |\underline{V}_R|$ and α_R are the normalized amplitude and phase of the open-circuit voltage, respectively; $N(t)$ is the number of multipath components, which is a function of the temporal variable t; and f is the frequency. The time dependency given through $e^{-j2\pi f\tau}$ is not explicitly shown in the above equation but the different delays of the various propagation paths is implicitly included in the phase α_R as will become apparent next.

Using $|\underline{V}_R| = \sqrt{P_R \cdot 8Re(\underline{Z}_R)}$ from (2.6) the open-circuit voltage in (3.1) can be written as:

$$\underline{V}_R(f,t) = \sqrt{P_R \cdot 8Re(\underline{Z}_R)} \cdot \sum_{i=1}^{N(t)} A_i(f,t)e^{j\phi_i(f,t)} \cdot e^{-j2\pi f\tau_i(t)} \tag{3.2}$$

where $A_i(f,t)$ and $\phi_i(f,t)$ are the amplitude and phase of the i-th multipath components which take into account the wave propagation effect; and τ_i is the delay of the i-th component. Thus, in general the amplitudes and phases of all individual multipath signals as well as the number of signals vary in time. Note that the above formulation assumes the time variable τ, while the temporal changes of the channel properties are associated to the variable t.

For the following discussion, we distinguish between *multipath fading* (i.e., *small-scale fading*) caused by moving the receiver through a dense spatial interference pattern, and the *fading of the local mean* (i.e., *large-scale fading*) due to slow temporal changes in the propagation environment (e.g., weather conditions, movement of the receiver from a LOS into a NLOS location). Small- and large-scale fading have been illustrated in Fig. 2.1.

3.2.1 Small-Scale Fading Distribution

Considering now only small-scale fading (i.e., the time-varying local mean has been already removed), the open-circuit voltage phasor can then be written as a summation

$$\underline{V}_R = V_R e^{j\alpha_R} = \sum_{i=1}^{N} V_{Ri}e^{j\alpha_{Ri}} = V_{R1}e^{j\alpha_{R1}} + \sum_{i=2}^{N} V_{Ri}e^{j\alpha_{Ri}} \tag{3.3}$$

of a constant number of N multipath signals, where the first term has been taken out of the summation to emphasized this component as will be explained below.

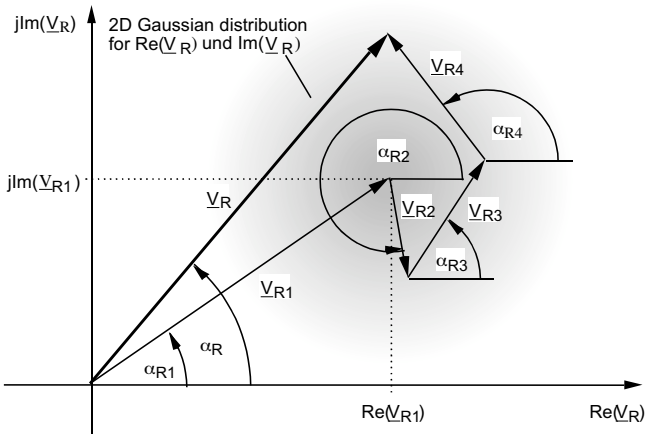

Figure 3.1: Linear superposition of a constant (deterministic) phasor $\underline{V}_{R1}$ and a large number of statistically independent, time-varying voltage phasors $\underline{V}_{Ri}$

The vector sum in (3.3) is illustrated in Fig. 3.1. Assuming a *constant (deterministic) phasor* $\underline{V}_{R1}$ and a large number of *statistically independent* signals $i = 2, \ldots N$ of *similar magnitude* and statistically varying phases. The complex (real and imaginary part) open-circuit voltage $\underline{V}_R$ is characterized by a *two-dimensional Gaussian distribution* (central limit theorem [Papoulis, 1984]).

Most often we are not interested in the two-dimensional probability density function (pdf) of the complex open-circuit voltage, but only in the one-dimensional pdf for the magnitude. Starting from the 2D-Gaussian distribution, the pdf *for the magnitude* can be derived by an integration over the phase from 0 to 2π, resulting in the *Ricean distribution* [Rappaport, 1996]

$$p(V_R) = \frac{V_R}{\sigma^2} I_0\left(\frac{V_{R1} V_R}{\sigma^2}\right) e^{-\frac{V_{R1}^2 + V_R^2}{2\sigma^2}} \quad \text{with} \quad \sigma^2 = \frac{1}{2}\overline{\left|\sum_{i=2}^{N} \underline{V}_{Ri}\right|^2} = \frac{1}{2}\sum_{i=2}^{N} \overline{V_{Ri}^2}, \tag{3.4}$$

where $I_0(x)$ denotes the modified Bessel function of zero order [Abramowitz, 1972].

The Ricean distribution (3.4) is often described in terms of the so-called *Ricean factor*

$$K = \frac{V_{R1}^2/2}{\sum_{i=2}^{N} \overline{V_{Ri}^2}/2} = \frac{V_{R1}^2}{2\sigma^2} \tag{3.5}$$

which is defined as the ratio between the deterministic signal power and the variance of the multipath (i.e., the signal power of all remaining multipath signals), and which completely specifies the shape of the Ricean distribution. Therefore, the Ricean factor K is equivalent to a "signal-to-noise ratio" (SNR) for the "wanted" deterministic signal and the "unwanted" remaining multipath (equivalent noise). Fig. 3.2 shows the Ricean pdf for different values of the K-factor or SNR, respectively.

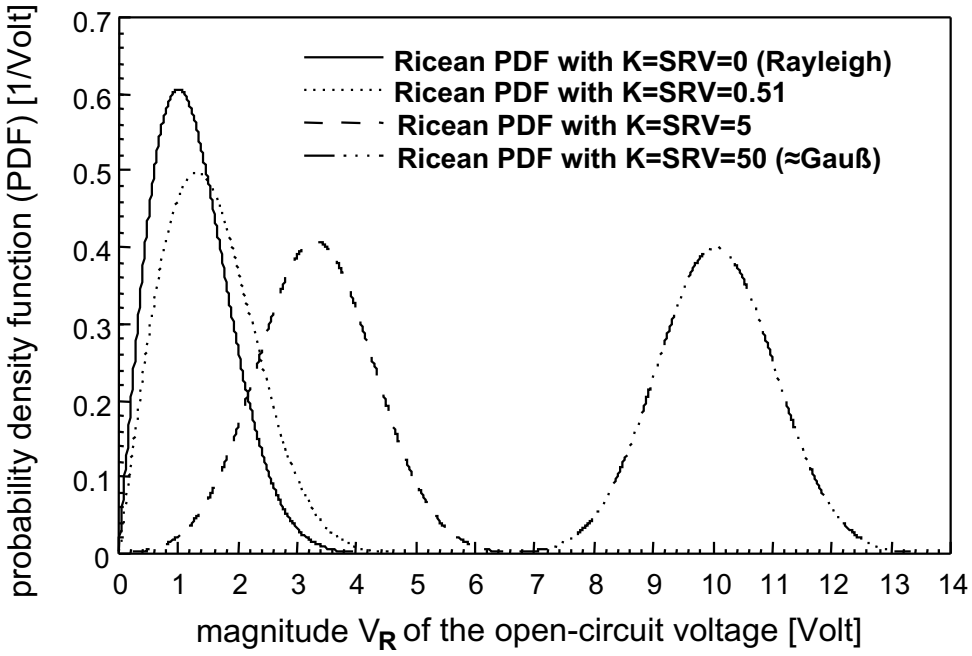

Figure 3.2: Ricean probability density function (pdf) for different Rice factors K and a normalized variance $\sigma^2 = 1\mathrm{Volt}^2$, including the limiting cases of Rayleigh ($K = 0$) and Gaussian distribution ($K = \infty$)

For a vanishing deterministic signal $\underline{V}_{R1}$ (see limiting case $K = 0$ in Fig. 3.2), the more general Ricean distribution approaches the special case of a *Rayleigh distribution*. The Raleigh distribution is commonly used to describe the statistical time varying nature of the received signal envelope, when there is *no dominant stationary* (i.e., non-fading, deterministic) *signal* component, such as a line-of-sight propagation path. The Rayleigh pdf [Rappaport, 1996]

$$p(V_R) = \frac{V_R}{\sigma^2} e^{-\frac{V_R^2}{2\sigma^2}} \tag{3.6}$$

directly follows from the Ricean pdf in (3.4) for V_{R1}=0, where σ is the RMS value of the received voltage signal, and σ^2 is the time-averaged power of the signal.

On the other hand, the Ricean distribution approaches the *Gaussian probability density function* for a dominant deterministic signal (e.g., for a LOS signal much stronger than all remaining signals). In this case the pdf is given by:

$$p(V_R) \approx \frac{1}{\sqrt{2\pi}\sigma} e^{-\frac{(V_R - V_{R1})^2}{2\sigma^2}} \quad \text{for} \quad K = \frac{V_{R1}^2}{2\sigma^2} \to \infty \tag{3.7}$$

where this second limiting case of the Ricean distribution is also shown in Fig. 3.2.

Drill Problem 24 *What is the condition on the random quantities $\underline{x}_i$ required for the equality*

$$\overline{\left|\sum_{j=1}^{M} \underline{x}_j\right|^2} = \sum_{j=1}^{M} \overline{x_j^2}, \tag{3.8}$$

to hold? Show that the above equality holds in this case. Relate this to the condition on the voltages $\underline{V}_{\mathrm{R}i}$ in (3.4)

Drill Problem 25 *Consider a multipath scenario with no dominant LOS contribution. The pdf in this case is given by the Rayleigh distribution. Calculate the probability that the open circuit voltage $V_R \geq 1.5\,\mathrm{V}$ given that the RMS value of the voltage is $\sigma = 0.9\,\mathrm{V}$. Explain why for this scenario the average value of the open circuit complex voltage $\underline{V}_R$ is zero (2D Gauss pdf) while the average power is larger than zero.*

Drill Problem 26 *Show that for a large Rican factor K (dominant line of sight component) the probability density function (pdf) of a Ricean distribution (given in (3.4)) can be approximated by a Gaussian pdf given by:*

$$p(V_R) \approx \frac{1}{\sqrt{2\pi}\sigma} e^{-\frac{(V_R - V_{R1})^2}{2\sigma^2}} \tag{3.9}$$

with V_R the total voltage; V_{R1} the dominant voltage; σ^2 the noise power; and $I_0(z)$ the modified Bessel function of the first kind and zero-order. Hint: For large arguments $|z|$ the modified Bessel function can be approximated by:

$$I_\nu(z) \approx \frac{e^z}{\sqrt{2\pi z}} \left(1 - \frac{\mu - 1}{8z} + \frac{(\mu - 1)(\mu - 9)}{2!(8z)^2} - \ldots\right) \tag{3.10}$$

where $\mu = 4\nu^2$ and ν is fixed.

3.2.2 Log-Normal Fading

Many simple large-scale propagation models (see chapter 2) do not consider the fact that the surrounding environmental may be vastly different at two different locations having the same T-R (transmit-receive) separation. This leads to measured signals often significantly different from the average values predicted by these propagation models. Measurements have shown that at a particular T-R distance d, the path loss $PL(d)$ is random and often *log-normally* (normal in dB) distributed about the mean distance-dependent value $PL(d)$ [Geng and Wiesbeck, 1998, Rappaport, 1996]. That is

$$p\left(\frac{PL}{\mathrm{dB}}\right) = \frac{1}{\sqrt{2\pi}\frac{\sigma_{PL}}{\mathrm{dB}}} \exp\left[-\frac{\left(\frac{PL}{\mathrm{dB}} - \frac{m_{PL}}{\mathrm{dB}}\right)^2}{2\left(\frac{\sigma_{PL}}{\mathrm{dB}}\right)^2}\right] \tag{3.11}$$

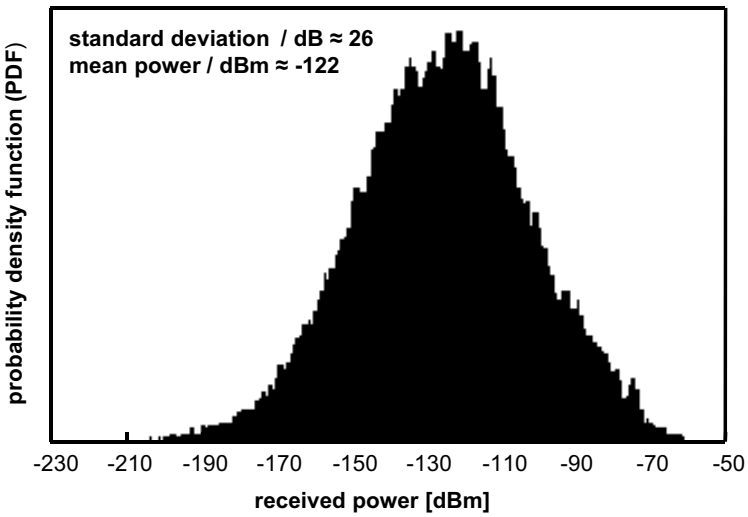

Figure 3.3: Calculated large-scale pdf for a GSM1800 coverage area of several square kilometers

where m_{PL}/dB and σ_{PL}/dB are mean and standard deviation of the path loss in dB, respectively.

The log-normal distribution describes the random shadowing effects which occur over a large number of measurement locations which have the same T-R separation, but different environment and obstruction and levels on the propagation path. Note that in (3.11), path loss, mean, and standard deviation are all measured in dB. Thus, the log-normal distribution is simply characterized by a Gaussian distribution when using dB-values.

In practice, the standard deviation is often computed using measured data (e.g., leading to about 7 dB to 10 dB for typical digital mobile radio systems like GSM). However, more sophisticated large-scale propagation models, like full wave models (e.g., integral equation methods, parabolic equation method) or ray-optical models are able to include detailed information on topography and land usage. Therefore, when using these more advanced large-scale wave propagation modeling techniques, there is no need to include an uncertainty region around the predicted path loss given by the measured standard deviation. Fig. 3.3 shows the large-scale pdf for a GSM1800 coverage area of several square kilometers, calculated using the Parabolic Equation Method [Geng and Wiesbeck, 1998]. As can be seen, the pdf for the received power in dB (and similar for the path loss in decibel) closely resembles a Gaussian distribution, i.e., the magnitude of the received voltage is log-normally distributed.

3.3 Channel Transfer Function and Impulse Response

The small-scale variations of a radio signal can be directly related to the impulse response of the radio channel. The impulse response is a wideband channel characterization and contains all information necessary to simulate or analyze any type of radio transmission. This stems from the fact that a radio channel may be modelled as a linear filter with a *time varying impulse response* $h(\tau, t)$, where the temporal variation (described by the variable t) is due to spatial receiver motion or time-varying propagation conditions (e.g., moving obstacles, weather conditions). Alternatively, the radio channel can be characterized by the Fourier transform of the impulse response, i.e., the time-varying channel transfer function $\underline{H}(f, t) = \mathcal{F}_\tau\{h(\tau, t)\}$.

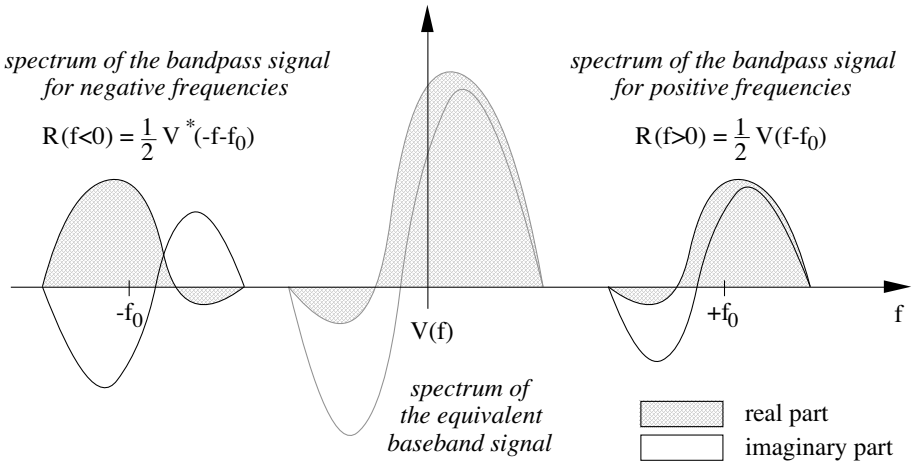

Figure 3.4: Spectrum $\underline{R}(f)$ of a real-valued bandpass signal $r(\tau)$ and corresponding equivalent baseband spectrum $\underline{R}(f)$ for a reference frequency of f_0

The spectrum of the signal transmitted by a general radio communication system is necessarily bandlimited to the vicinity of a carrier of frequency f_0. Note that antennas cannot effectively radiate energy for wavelengths significantly larger than the antenna dimensions, thus, the spectrum does not contain a DC component. Such, necessarily real-valued *bandpass signals* are favorably described by *equivalent baseband* or low-pass *signals* (sometimes called *complex envelope*) or corresponding *equivalent baseband spectra* (Figs. 3.4 and 3.6) [Papoulis, 1977]. The time-varying channel transfer function $\underline{H}(f, t)$ of the radio channel is given by:

$$\underline{H}(f, t) = \frac{1}{2}\underline{C}(f - f_0, t) + \frac{1}{2}\underline{C}^*(-f - f_0, t) \tag{3.12}$$

and its inverse Fourier transform, the real-valued impulse response $h(\tau, t)$ written as

$$\begin{aligned} h(\tau,t) &= \frac{1}{2}\underline{c}(\tau,t)e^{+j2\pi f_0\tau} + \frac{1}{2}\underline{c}^*(\tau,t)e^{-j2\pi f_0\tau} \\ &= Re\left\{\underline{c}(\tau,t)e^{+j2\pi f_0\tau}\right\} \\ &= |\underline{c}(\tau,t)|\, cos(2\pi f_0\tau + \angle\underline{c}(\tau,t)) \end{aligned} \tag{3.13}$$

where $\underline{c}(\tau,t) = \mathcal{F}_\tau^{-1}\{\underline{C}(f,t)\}$.

Drill Problem 27 *Fill out the empty fields in the table below indicating the input, channel, and output quantities in the various time and frequency representations. Indicate whether each quantity is real or complex and correctly assign the independent variables.*

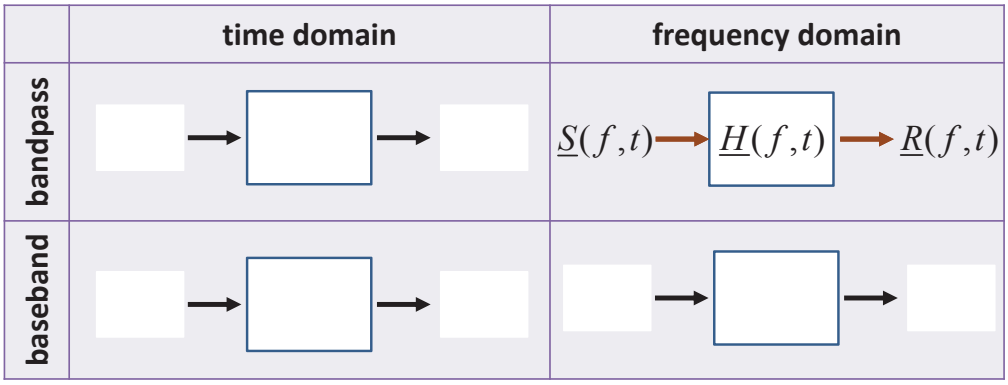

Figure 3.5: Representation of signals and systems in the time and frequency domain.

The channel impulse response is easily determined from the equivalent baseband response of the channel by a multiplication with $\exp j2\pi f_0\tau$ accounting for the high-frequency carrier and using the real value only (similar to the usage of complex phasors in time-harmonic analyses).

3.4 Characterization of Frequency-Selective Channels

Under several conditions (not given here for simplicity), the *equivalent baseband impulse response* (i.e., the complex envelope) of a radio transmission channel can be written as [Geng and Wiesbeck, 1998, Rappaport, 1996]

$$\underline{c}(\tau,t) = \sum_{i=1}^{N(t)} b_i(t)e^{j\phi_i(t)}\delta\left[\tau - \tau_i(t)\right] \tag{3.14}$$

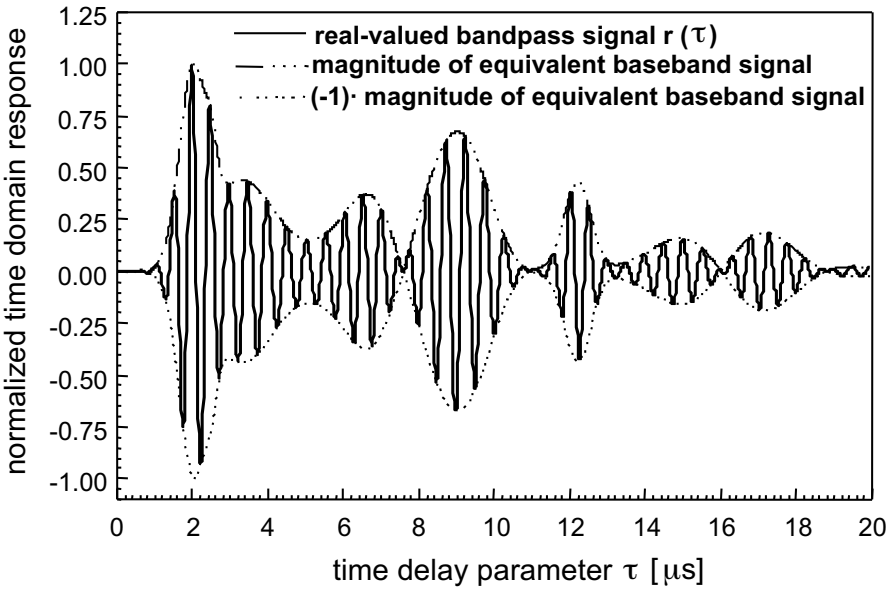

Figure 3.6: Real-valued bandpass signal $r(\tau)$ and corresponding magnitude of the equivalent (complex-valued) baseband/lowpass signal $\underline{v}(\tau)$.

which is intuitively clear. The received signal for an impulse $\delta(\tau)$ exciting the multipath channel (i.e., the impulse response) consists of a *series of attenuated*, *phase-shifted*, and *time-delayed replicas* of the transmitted signal. In reality, however, the channel is always bandlimited. Thus, the Dirac impulses in (3.14) have to be replaced by some filter function characterizing the finite bandwidth of the channel. Fig. 3.7 shows an example for the idealized impulse response, or more strictly speaking, the magnitude of the equivalent baseband response (i.e., the envelope), together with more realistic bandlimited versions. The latter can be measured by channel sounding techniques (in the frequency or time domain) [Rappaport, 1996].

Now the dispersive, i.e. frequency dependent, radio channel can be characterized either in the time or in the frequency domain using the impulse response or the channel transfer function, respectively. However, in all practical situations the propagation channel is varying in time and space, i.e. when measuring the channel transfer function or the impulse response at different spatial locations and/or different times, the results will be different. Therefore the description has to be based on statistical methods.

Time Domain Characterization

In the time domain, the characterization of the dispersive radio channel is most often based on the so-called *Power Delay Profile* (PDP) defined as [Geng and Wiesbeck, 1998,

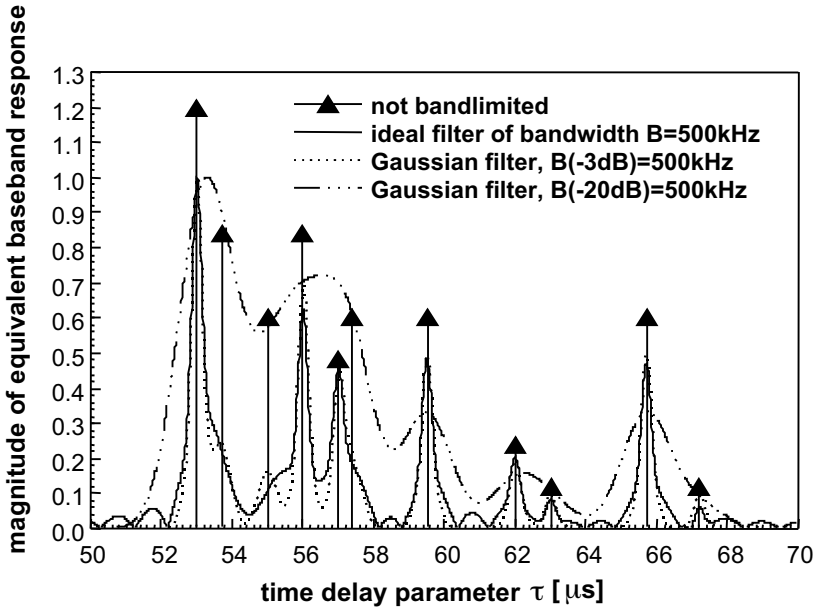

Figure 3.7: Magnitude of the (complex) equivalent baseband impulse response for the case of infinite bandwidth compared to those using ideal and Gaussian band limitation.

Rappaport, 1996]

$$PDP(\tau, t) = K \cdot |\underline{c}(\tau, t)|^2 \tag{3.15}$$

and shown in Fig. 3.8 which describes the relative received power as a function of the delay.

By making several local measurements of the PDP at different spatial (or temporal) locations, it is possible to build an ensemble of PDPs, each one representing a possible small-scale multipath channel state. Therefore, many snapshots of $PDP(\tau, t)$ are averaged to provide a time-invariant multipath power delay profile $PDP(\tau)$ (i.e., *mean PDP*). The parameter K in (3.15) relates the total transmitted power (contained in the probing pulse) to the total received power of the PDP and is irrelevant in the current context.

In order to compare different multipath channels and to develop some general design guidelines for wireless systems, parameters which grossly quantify the multipath channel are utilized. The mean excess delay and the RMS delay spread are multipath channel parameters that can be determined directly from a PDP. The *mean excess*

delay is the first moment of the PDP and is defined as

$$\overline{\tau} = \frac{\int_{-\infty}^{+\infty} \tau \cdot PDP(\tau) d\tau}{\int_{-\infty}^{+\infty} PDP(\tau) d\tau} \tag{3.16}$$

The *RMS delay spread* is the square root of the second central moment of the PDP defined by

$$\tau_{DS} = \sqrt{\overline{(\tau - \overline{\tau})^2}} = \sqrt{\overline{\tau^2} - \overline{\tau}^2} = \sqrt{\frac{\int_{-\infty}^{+\infty} \tau^2 \cdot PDP(\tau) d\tau}{\int_{-\infty}^{+\infty} PDP(\tau) d\tau} - \left(\frac{\int_{-\infty}^{+\infty} \tau \cdot PDP(\tau) d\tau}{\int_{-\infty}^{+\infty} PDP(\tau)\, d\tau} \right)^2} \tag{3.17}$$

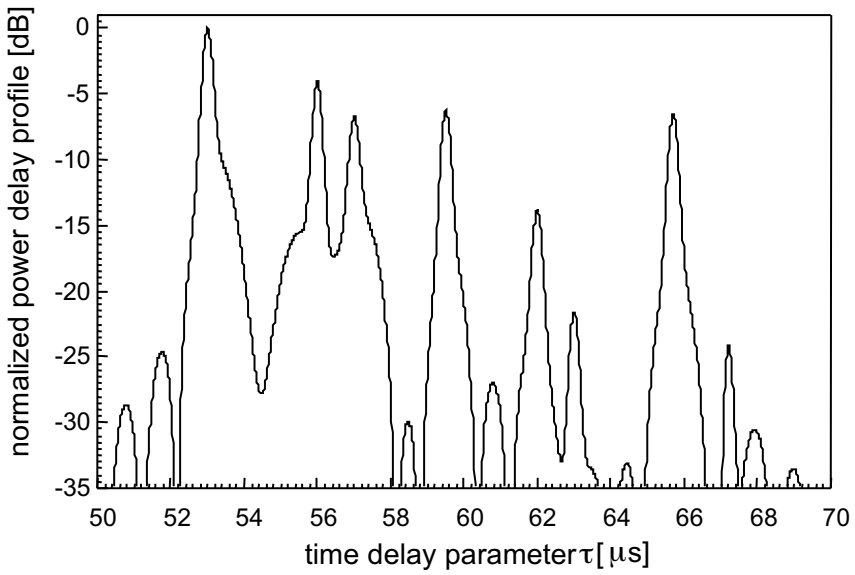

Figure 3.8: Normalized power delay profile (PDP) (in log-scale) for the strictly bandlimited case in Fig. 3.7 (i.e., with ideal filter of bandwidth $B = 500\,\text{kHz}$)

Equations (3.16) and (3.17) do not rely on the absolute power level of the PDP, but only on relative amplitudes of the multipath components within $PDP(\tau)$. Typical values of the RMS delay spread are on the order of microseconds in outdoor mobile radio channels, on the order of nanoseconds in indoor radio channels, and several tens of nanoseconds for fixed-terminal microwave LOS radio links. It is important to note that the RMS delay spread and mean excess delay can be defined from a single PDP or the spatial/temporal average of PDPs resulting from consecutive impulse response

measurements. In the first case, measurements are made at many locations or times in order to determine a statistical range of multipath channel parameters for a radio communication system.

Frequency Domain Characterization

Although the power delay profile and the corresponding characteristic parameters are widely used, it seems to be more natural to describe the frequency-dependent (i.e., dispersive) radio channel directly in the frequency domain. The *Frequency Auto-Correlation Function* ACF_f defined as [Cox and Leck, 1975]

$$ACF_f(\Delta f, t) = \int_{-\infty}^{+\infty} \underline{C}(f,t)\,\underline{C}^*(f-\Delta f, t)\,df = \underline{C}(\Delta f, t) * \underline{C}^*(-\Delta f, t) \tag{3.18}$$

is used, which is directly based on the (equivalent baseband) channel transfer function $\underline{C}(f,t) = \mathcal{F}_\tau\{\underline{c}(\tau,t)\}$. The last equality gives the equivalent expression in terms of the *convolution* (symbol $*$) between two functions.

The frequency ACF quantifies over which range of frequencies the radio channel can be considered “flat” (for magnitude of the normalized frequency ACF close to unity), and for which frequency separation Δf there may be large differences in the channel transfer function.

The *parameter* used to describe the width of the frequency ACF is the *coherence or correlation bandwidth* $B_{corr,x\%}$. Fig. 3.9 shows three different transfer functions and the corresponding frequency ACF. Increasing frequency selectivity (i.e., faster variation of the transfer function with frequency) narrows the frequency ACF shown in Fig. 3.9b; and the coherence bandwidth decreases.

Relate Description in Time and Frequency Domain

According to the known theorems of the Fourier transform [Papoulis, 1962], the power delay profile (3.15) and the frequency ACF (3.18) constitute a pair of Fourier transforms (*Wiener-Khintchine theorem*).

$$ACF_f(\Delta f, t) = \mathcal{F}_\tau\{PDP(\tau, t)\} \tag{3.19}$$

Therefore, the width of the PDP characterized by the delay spread τ_{DS} and the width of the frequency ACF characterized by $B_{corr,x\%}$ satisfy the (*time-bandwidth product*) [Papoulis, 1977]

$$\tau_{DS} \cdot B_{corr,x\%} = const \quad \text{or} \quad B_{corr,x\%} \sim \frac{1}{\tau_{DS}} \tag{3.20}$$

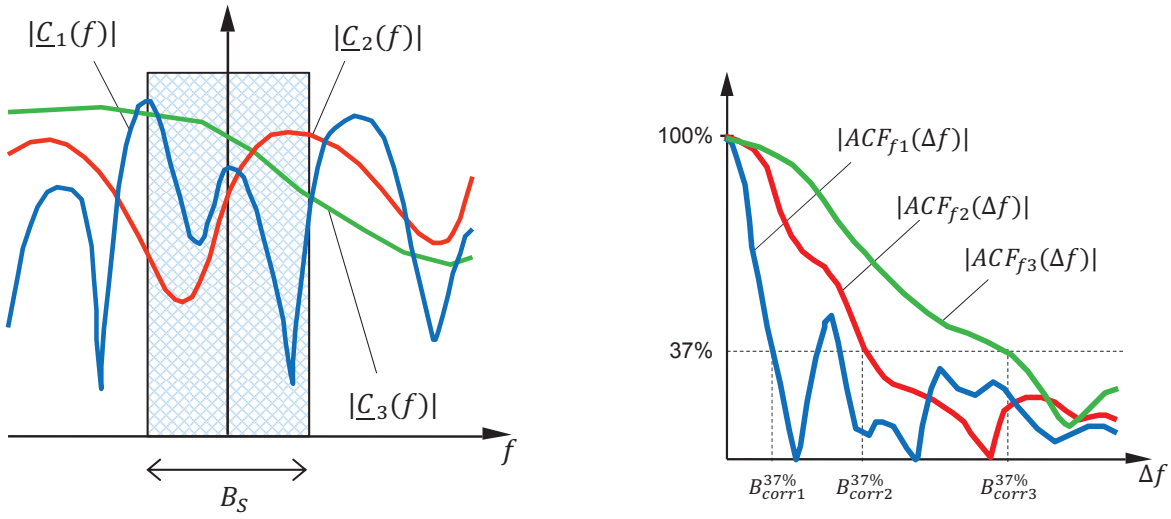

(a) channel transfer function

(b) frequency ACF

Figure 3.9: Comparison of three channel transfer functions and the corresponding frequency ACFs. The frequency variation is decreasing from case 1 to 3

where $const$ depends on the definition of the coherence bandwidth.

For the three different transfer functions and the corresponding frequency ACF shown in Fig. 3.9, this means that a decreasing coherence bandwidth correspondes to an increased delay spread as given in to (3.20). Frequency selective radio channels are therefore characterized by small coherence bandwidths and large delay spreads (see the following more detailed discussion).

Relate Channel to Signal

If the channel shows a constant-gain and linear-phase response only over a bandwidth that is smaller than the bandwidth B_S of the *transmitted signal*, then the channel creates *frequency selective fading*. Under such conditions, the impulse response has a multipath delay spread which is greater than the symbol period of the transmitted waveform (the symbol period and signal bandwidth are related through $T_S \sim 1/B_S$), and the received signal includes multiple versions of the transmitted waveform which are attenuated and delayed in time. Hence, the signal is distorted and the channel induces *intersymbol interference*.

On the other hand, if the transmitted signal bandwidth B_S is smaller then the coherence bandwidth of the radio channel, then the received signal will undergo *flat fading* (frequency-independent fading). The strength of the received signal still changes with time, but the changes are almost identical over the entire transmitted bandwidth.

To summarize, a signal undergoes *flat fading* if

$$B_S \ll B_{corr,x\%} \quad \text{or} \quad T_S \gg \tau_{DS} \tag{3.21}$$

and *frequency selective fading* if

$$B_S > B_{corr,x\%} \quad \text{or} \quad T_S < \tau_{DS} \tag{3.22}$$

Drill Problem 28 *Calculate the mean excess delay and the rms delay spread for the multipath profile given in Fig. 3.10. Then estimate the* $50\,\%$ *coherence bandwidth (i.e. the bandwidth where the related correlation function is above* 0.5*) of the channel.*

Would this channel be suitable for a mobile phone system occupying a channel bandwidth of 30 kHz *and/or GSM services with* 200 kHz *bandwidth?*

Hint: The constant $const$ *of time-bandwidth product equals* $1/50$ *for a correlation value above* 0.9*. If the demand of such a strong correlation is relaxed to* 0.5 *then* $const$ *can be assumed to be* $1/5$*.*

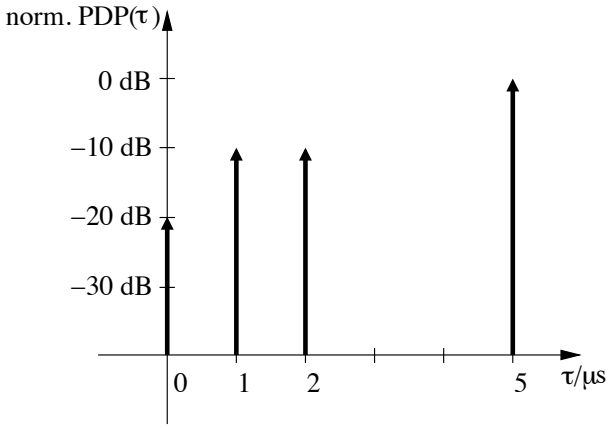

Figure 3.10: Normalized power delay profile.

3.5 Characterization of Time-Variant Channels

Delay spread and coherence bandwidth are parameters which describe the dispersive nature of the radio channel. However, they do not offer information about the time varying nature of the channel caused by either relative motion between MS and BS, or by movement of scattering objects. *Doppler spread* and *coherence time* are parameters which describe the time varying nature of the channel in a small-scale region [Geng and Wiesbeck, 1998, Rappaport, 1996].

With a pure sinusoidal tone $s(\tau) = V_0 cos(2\pi f_0 \tau)$ of frequency f_0 as input, the time-varying nature of the radio channel results in an output which is no longer a pure harmonic signal:

$$\begin{aligned} r(\tau,t) &= V_0 \left|\underline{H}(f_0,t)\right| \cos\left[2\pi f_0 \tau + \angle(\underline{H}(f_0,t))\right] \\ &= \frac{1}{2} V_0 \left|\underline{C}(0,t)\right| \cos\left[2\pi f_0 \tau + \angle(\underline{C}(0,t))\right] \end{aligned} \tag{3.23}$$

where $r(\tau,t)$ can also be written as

$$r(\tau) = Re\left\{\underline{v}(t) e^{j2\pi f_0 \tau}\right\} \tag{3.24}$$

with the time-varying complex envelope $\underline{v}(t)$ of the output signal.

Time Domain Characterization

Statistically, this time-varying nature of the radio channel can be represented by the temporal Auto-Correlation Function:

$$ACF_t(\Delta t) = \int_{-\infty}^{+\infty} \underline{v}(t)\underline{v}^*(t-\Delta t)dt = \underline{v}(\Delta t) * \underline{v}^*(-\Delta t) \tag{3.25}$$

with $*$ being the convolution. Note that both $\underline{v}(t)$ and $ACF_t(\Delta t)$ are functions of the variable t indicating the temporal changes (the time variable τ does not appear in the equations).

The temporal ACF is often described by a single parameter called *coherence time* (or correlation time) $T_{corr,x\%}$ defined similar to the coherence bandwidth (section 3.4). Here the correlation time is an indication over which time intervals the envelope and by this the channel can be considered constant. Fig. 3.11 clarifies the relation between the temporal envelope variation on one side and the related autocorrelation function and coherence time on the other.

Frequency Domain Characterization

The power spectral density (PSD) of the time-varying complex envelope $\underline{v}(t)$ is

$$PSD(f_D) = \left|\mathcal{F}_t\{\underline{v}(t)\}\right|^2 = \left|\int_{-\infty}^{+\infty} \underline{v}(t) e^{-j2\pi f_D t} dt\right|^2 = \left|\underline{V}(f_D)\right|^2 \tag{3.26}$$

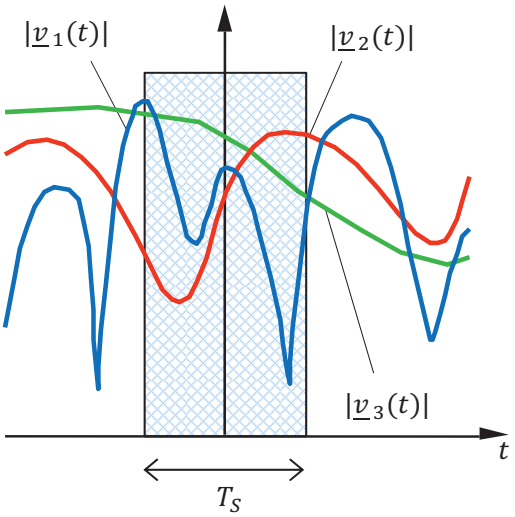

(a) time varying envelope

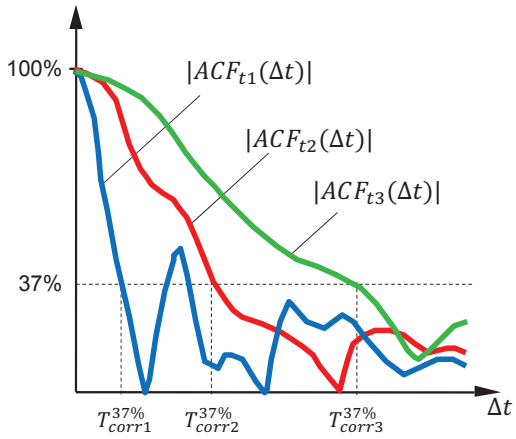

(b) temporal ACF

Figure 3.11: Comparison of three time-varying envelope functions and the corresponding temporal ACFs. Case 1 has the fastest temporal variation.

where f_D is the Doppler frequency[1] for which $PSD(f_D)$ is also called *power Doppler spectrum* . The power spectra of the transmitted and received signals are illustrated in Fig. 3.12.

The parameter used to describe the PSD is the *Doppler spread* B_{DS} defined by:

$$B_{DS} = 2\sqrt{\overline{f_D}^2 - \overline{f_D}^2} = 2\sqrt{\frac{\int_{-\infty}^{+\infty} f_D^2 \cdot PSD(f_D)df_D}{\int_{-\infty}^{+\infty} PSD(f_D)df_D} - \left(\frac{\int_{-\infty}^{+\infty} f_D \cdot PSD(f_D)df_D}{\int_{-\infty}^{+\infty} PSD(f_D)df_D}\right)^2} \tag{3.27}$$

The Doppler spread is a measure of the spectral broadening caused by the time rate of change of the mobile radio channel and therefore a measure for the range of frequencies over which the PSD is essentially non-zero. The Doppler shift $\overline{f_D}$ on the other hand gives an indication of the average or mean frequency of the PSD.

Drill Problem 29 *Write an expression to define the Doppler shift* $\overline{f_D}$ *from the power spectral density (power Doppler spectrum)* $PSD(f_D)$.

[1] Note that the Fourier transform with respect to t is represented by the f_D, while the Fourier transform with respect to τ gives f.

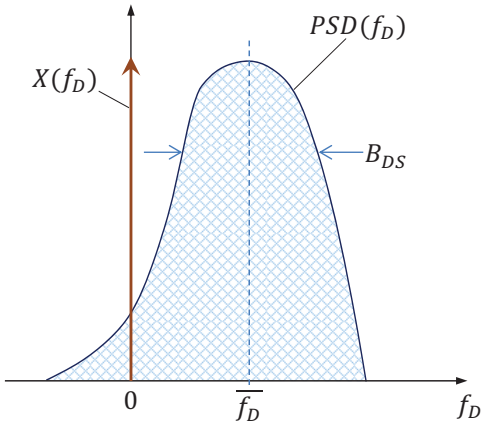

Figure 3.12: Power spectral density function of the received radio signal for a pure sinusoidal transmitted signal.

Relate Description in Time Frequency Domain

According to the theorem of Wiener-Khintchine, the Fourier transform of the ACF (3.28) yields:

$$\mathcal{F}_t\{ACF_t(\Delta t)\} = \mathcal{F}_t\{\underline{v}(\Delta t) * \underline{v}^*(-\Delta t)\} = \underline{V}(f_D)\underline{V}^*(f_D) = |\underline{V}(f_D)|^2 = PSD(f_D) \quad (3.28)$$

Due to the fact that temporal ACF and power Doppler spectrum form a Fourier pair, the product of coherence time (characterizing the width of the ACF) and the Doppler spread (characterizing the width of the Doppler spectrum) is constant (*time-bandwidth product*) [Rappaport, 1996], i.e.,

$$T_{corr,x\%} \cdot B_{DS} = const \quad \text{or} \quad T_{corr,x\%} \sim \frac{1}{B_{DS}} \quad (3.29)$$

Relate Signal to Channel

The coherence (correlation) time is a statistical measure of the time duration over which the channel is essentially invariant. In other words, the coherence time is the time separation for which received signals have a strong potential for amplitude correlation. If the symbol period of the transmitted signal T_S is greater than the coherence time, then the channel will change during the transmission of a single symbol, thus causing distortion.

On the other hand, if the symbol period is much smaller than the coherence time, or equivalently, if the signal bandwidth is much larger than the Doppler spread, the

effects of Doppler spread are negligible. In summary, depending on how rapidly the transmitted baseband signal varies compared to the rate of change in the channel characteristics, a radio channel may be classified either as a *fast fading* or *slow fading* channel. The signal undergoes *slow fading* if

$$T_S \ll T_{corr,x\%} \quad \text{or} \quad B \gg B_{DS} \tag{3.30}$$

and it is characterized as *fast fading* if

$$T_S > T_{corr,x\%} \quad \text{or} \quad B < B_{DS} \tag{3.31}$$

It should be noted that when a channel is specified as a slow- or fast-fading channel, it does not specify whether the channel is flat fading or frequency selective in nature. In the case of a flat-fading channel, we can approximate the impulse response to be simply a single delta function. Hence, for a *flat-fading and fast-fading* channel, the amplitude of the delta function varies faster than the rate of change of the transmitted baseband signal. In case of a *frequency-selective and fast-fading* channel, the amplitudes, phases, and time delays of all multipath signals vary faster than the rate of change of the transmitted signal.

Drill Problem 30 *A channel is characterized by a delay spread* $\tau_{DS} = 18\,\mu\text{s}$ *and a Doppler spread* $B_{DS} = 105\,\text{Hz}$*. The channel is used to transmit a GSM-signal which has a bandwidth of* $200\,\text{kHz}$*.*
i) How is the correlation bandwidth B_{corr} *related to the parameters mentioned above?*
ii)How is the correlation time T_{corr} *related to the parameters mentioned above?*
iii) What types of small-scale fading will a GSM-signal experience in the channel?

3.5.1 Doppler Spectrum of Received Signal

In a multipath environment where the receiver is moving at a velocity ν_R, each path i will have a distinct Doppler frequency shift $\overline{f_{Di}}$ given by:

$$\overline{f_{Di}} = \frac{|\nu_R| \cos\alpha_i}{c_0/f_0} = \frac{|\nu_R| \cos\alpha_i}{\lambda_0} = \frac{|\nu_{R,\text{radial}}|}{\lambda_0} \qquad i = 1, 2, \ldots, N \tag{3.32}$$

where α_i is the angle between the velocity vector ν_R and the direction of arrival of path i, and N is the total number of multipath components.

Drill Problem 31 *Consider a stationary transmitter which radiates a sinusoidal carrier frequency of* $1850\,\text{MHz}$*. Compute the received carrier frequency if the receiver is mounted in a car moving at* $\nu_R = 130\,\text{km h}^{-1}$*.*

i) directly towards the transmitter.
ii) directly away from the transmitter.
iii) perpendicular to the direction of arrival of the signal.

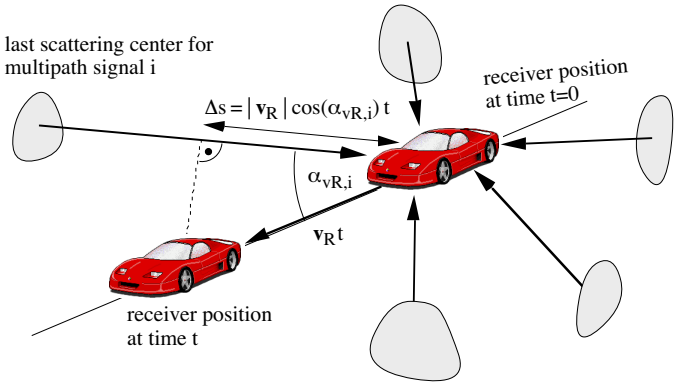

Figure 3.13: Typical geometry for the multipath wave propagation in a mobile radio system with a moving receiver at speed V_R.

However, the spectrum of the received signal (at the terminals of the antenna) will have spectral components in the range between $f_0 - f_{Dmax}$ and $f_0 + f_{Dmax}$, where f_{Dmax} is the maximum Doppler shift. The amount of broadening depends on the relative velocity of the mobile receiver and the angle α_i between the directions of MS motion and incoming multipath signals as can be seen from Fig. 3.13.

In mobile radio communication systems for urban areas, the Doppler spectrum is often approximately characterized by the *Jakes spectrum* [Jakes, 1974] which is illustrated in Fig. 3.14 for a GSM/DCS1800 system (carrier frequency $f_0 = 1800\,\text{MHz}$) and a mobile receiver travelling at a speed of $\nu_R = 130\,\text{km}\,\text{h}^{-1}$, resulting in a maximum Doppler frequency of $f_{Dmax} = v_R/\lambda_0 = 217\,\text{Hz}$.

Drill Problem 32 *A relative motion of a receiver to a transmitter leads to a Doppler shift of the received frequency. If the incidence angles at the receiver are equally distributed one can find a continues Doppler spectrum.*

i) Derive the formula to calculate the Doppler shift for a moving receiver.

ii) Show that the Doppler spectrum can be described by a Jakes spectrum

$$\Psi\left(f_D\right) = \frac{\text{const}}{\pi f_{D,max}\sqrt{1-\left(\frac{f_D}{f_{D,max}}\right)^2}} \tag{3.33}$$

if the incidence angles and the amplitudes are equally distributed.

iii) Determine the mean Doppler shift $\overline{f_D}$ and the Doppler spread B_{DS}.

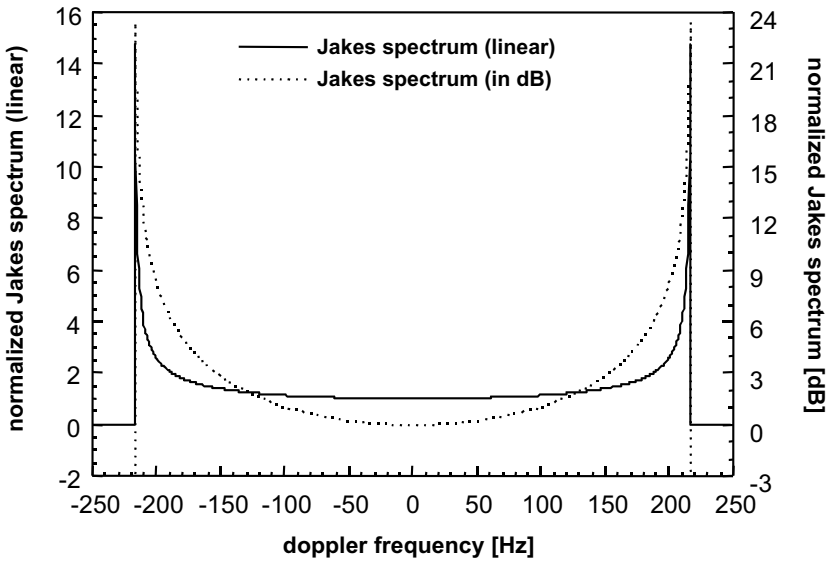

Figure 3.14: Jakes Doppler spectrum for a mobile receiver travelling at a speed of $130\,\mathrm{km\,h^{-1}}$ in a GSM/DCS1800 mobile system $f_0 = 1800\,\mathrm{MHz}$.

Bibliography

[Abramowitz, 1972] Abramowitz, M. (1972). *Handbook of Mathematical Functions*. Dover Publ.

[Cox and Leck, 1975] Cox, D. and Leck, R. (1975). Correlation bandwidth and delay spread multipath propagation statistics for 910 mhz urban mobile radio channels. *IEEE Transactions on Communications*, 23:1271–1280.

[Geng and Wiesbeck, 1998] Geng, N. and Wiesbeck, W. (1998). *Planungsmethoden für die Mobilkommunikation - Funknetzplanung unter realen physikalischen Ausbreitungsbedingungen*. Springer.

[Jakes, 1974] Jakes, W. (1974). *Microwave Mobile Communications*. Wiley.

[Papoulis, 1962] Papoulis, A. (1962). *The Fourier Integral and its Applications*. McGraw-Hill.

[Papoulis, 1977] Papoulis, A. (1977). *Signal Analysis*. McGraw-Hill.

[Papoulis, 1984] Papoulis, A. (1984). *Probability, random variables, and stochastic processes*. McGraw-Hill, 2 edition.

[Rappaport, 1996] Rappaport, T. (1996). *Wireless Communications*. Prentice Hall.